

# A Study on Cylindrical Coil Spring Deflection and Stress Done Using Analytical and Numerical Methods

Damjan Čakmak, Zvonimir Tomičević, Ivo Senjanović, Hinko Wolf, Željko Božić, Damir Semenski

University of Zagreb, Faculty of Mech. Eng. and Nav. Arch., 10 000 Zagreb, CROATIA  
e-mail (corr. author): damjan.cakmak@fsb.hr

## SUMMARY

*In this study, a linear cylindrical coil spring under axial quasi-static point load is considered. Two types of coil springs with a circular cross-section, i.e. straight and inclined, are clearly distinguished and analysed. The straight cross-section implies parallelism with respect to the vertical axis of the spring. The inclined cross-section considers the perpendicularity with respect to the tangent of the spring helix curve. Several new closed-form spring deflection and stress correction factors are proposed which constitutes the main contribution of this manuscript. The obtained results are based on the basic theory of strength of materials, the theory of elasticity, and linear finite element analysis. The novel correction factors prove to be very accurate compared to the parametric numerical analyses performed and the results obtained from the literature. The accuracy of the proposed corrections is especially evident when considering very large pitch angles in combination with small spring indices, i.e. thick and steep coil springs. The direct engineering applicability of the obtained results is highlighted.*

**KEY WORDS:** *cylindrical coil spring; deflection correction factor; stress correction factor; finite element method.*

## 1. INTRODUCTION

Spring is one of the most important mechanical components used in engineering applications. Mechanical springs are fundamental elements of modern machines and devices [1]. The most common type of spring is the cylindrical coil spring with a circular cross-section, or in short – the helical spring. It is commonly used in various shapes and sizes, from retractable pens and pencils to vehicle suspensions [2].

The basic theory of calculating the deflection and stress of the coil spring, usually given in textbooks on the strength of materials (SOM) [3]-[5] or on machine design [6]-[8], is based on the assumption that spring can be considered as a straight bar under pure torsion [9]-[11]. This assumption is approximately true if the spring index  $C$  is large (if the spring is a slender one) and if the initial helix pitch angle  $\alpha$  is small [1],[11]. For tension springs, the small pitch

angle condition is usually satisfied [1]. However, for compression springs, the pitch angle tends to become larger [5]. Such springs are usually referred to as open coil springs [1],[5]. Moreover, in heavy/thick industrial spring applications [1],[4], the spring index tends to smaller values and the simplified straight bar assumptions no longer apply [12]. Consequently, the most stressed area is normally on the inner side of the helix due to the shift of the neutral line [1],[4]-[6]. This is particularly important for the assessment of the spring fatigue life [1],[6]. Timoshenko readily acknowledged that cracks in cyclically loaded heavy springs usually start on the inner side of the coil [4]. If the conditions of large spring index and small pitch angle are not satisfied simultaneously, the estimated results of simplified calculations may largely deviate from the realistic spring deflection and stress [1]-[18]. Hence, there is a need to more accurately capture the spring behaviour under load. This led to the further development of simple analytical approximation models, first introduced by Love [19], which aim to provide sufficiently accurate estimations for spring deflection and stress.

Pioneering works in this field are by Wahl [1],[11],[20], Göhner [1],[21],[22], Henrici [23],[24], Ancker and Goodier (A/G) [12],[15], Bergsträsser [15],[25] and by many other authors [15]-[18]. The often cited systematic studies on spring correction factors by Göhner, [1],[5],[15],[25]-[27], are of particular importance. As a basis for his work, Göhner used the theory of elasticity (TOE) and a number of approximations to obtain highly accurate stress correction factors, even by today's standards [16],[17]. Consequently, the old German DIN standard (now defunct) for the calculation and design of cylindrical helical springs [28],[29] was based on Göhner's correction. Henrici [23] was directly influenced by Göhner in deriving his approximate stress correction factor using the Legendre power series function. Their joint results agree well up to the second order approximation [25]. Ancker and Goodier [12] also relied on Göhner's results and additionally considered pitch angle effects with a slightly different implementation than Göhner [1]. The authors derived detailed equations for the deflection and stress in a helical spring using the TOE approach and the so-called thin-slice method [17],[27]. They used truncated, double infinite power series in the terms of the combined effects of spring index, coil curvature, and initial pitch/helix angle [12]. Ancker and Goodier additionally reported that the pitch angle contributes significantly to the strains/stresses. This was confirmed via FEM in [18]. However, their research methods raised some controversies. Lin and Pisano [30] state that some of the assumptions made in the A/G analysis limit their theory to infinitesimally small pitch angles (*e.g.*, it was assumed that the cross-section of the spring cut by a vertical plane always remains circular, which is further referred to as a straight cross-section), although the authors intended to analyse the case of the large pitch angle. Nevertheless, the A/G correction factors are regularly included in modern engineering textbooks [3] and are particularly widely used in nano-spring technology [31]-[33]. Furthermore, Wahl [1],[11] based his stress correction factor [14]-[18] on SOM assumptions. The author additionally used the Timoshenko shear correction factor derived for the shear stress at the horizontal edge of a cantilever circular beam [26]. Wahl [1] noted that his stress correction is more conservative compared to Göhner's [14]. He also reported that Göhner's correction is more accurate and in better agreement with the experimental analysis performed [1]. Moreover, it is important to acknowledge the Bergsträsser approximate/empirical stress correction factor [15]-[18] which indeed agrees quite well with the Göhner approximation. The new (current) DIN standard [34],[35] is simultaneously based on the Bergsträsser and the Wahl stress correction factor.

Due to complicated geometries and operating conditions of modern machine components, the analytical estimation of spring deflection/stress and the corresponding fatigue life is often

omitted [36], or rather rarely used [39], in favour of numerical methods [37],[38]. In such cases, the Wahl approximate stress correction is commonly used for fatigue life assessment [6],[8],[39]. However, the Wahl stress correction may be too conservative in the context of fatigue assessment [1]. Nowadays, spring analysis is almost exclusively performed either with software based on the finite element method (FEM) [13]-[15],[27],[36]-[41], or experimentally [13],[14],[39]-[42]. Ideally, both methods can be combined to allow a fair comparison and validation of the obtained results [13],[14],[40],[41]. FEM provides advanced capabilities for detailed spring modelling techniques, such as the sub-modelling used in [14]. This technique can be used to study a local part of a spring model with refined mesh, based on the FEM result of a global model with coarse mesh [37]. The main reason for using FEM in spring design is its ability to reduce errors caused by simplifying the governing equations [15],[36],[40], mainly by underestimating the influence of the pitch angle [14]. Thus, the main reasons for the engineering failure of springs can be the incorrect evaluation of deflection (for buckling collapse) and stress (for structural/fatigue collapse). However, simplified analytical methods are still mandatory, at least in the initial design stages, as a quick verification tool [14],[41]. For example, coil spring manufacturers use governing equations that are usually proprietary and confidential and therefore not available to the general public [14].

More recently, further attempts have been made to check the accuracy of well-established correction factors (Wahl, Göhner, Ancker and Goodier, *etc.*) and to provide more accurate closed-form correction factors [15]-[18]. FEM was used as the primary verification tool for the accuracy of the state of stress in loaded helical compression springs. The authors used the von Mises stress energy criterion [6] and incorporated the Wahl stress correction [1] in their approximate analytical model. They verified the proposed model by performing FEM analyses and validated it with experimental investigations. Furthermore, Yıldırım [43],[44] proposed new analytical spring deflection correction factors using the Timoshenko thick beam theory [45]-[49] with the Cowper shear correction [50] for arbitrarily large spring pitch angles and different cross-sections. The results proposed in [43] for a helical spring with a circular cross-section are very similar to those previously obtained by Dym [51] who used Castigliano's method and applied a general unit shear correction to his model. This approach is also adopted in the textbook by Shigley [6], although only for considering small pitch angles. There is a general consensus that the Timoshenko beam is generally more accurate [52] compared to the slender Euler-Bernoulli (E/B) beam [53]. However, the E/B beam is still widely used in analytical and numerical calculations [53] due to its relative simplicity and straightforward implementation. Moreover, it was noted in [17] that the use of the Timoshenko theory in the context of the helical spring may overestimate spring compliance. It was additionally reported that the Timoshenko beam-based results diverge from the TOE-based A/G deflection correction [12] and from the corresponding 3D continuum FEM results in the case of small spring indices [37],[38].

These concepts and their shortcomings are further investigated in this study. The study carried out here aims to provide efficient and accurate formulae for design engineers and structural engineers. The proposed spring deflection and stress corrections are provided in simple and approximate closed form. The main contribution of this paper is given as follows. Two types of helical springs with a circular cross section, *i.e.* straight and inclined, are clearly defined and analysed. The accuracy of the Wahl stress correction factor is evaluated and a basic modification to the standard formula is proposed. It is confirmed that the Timoshenko beam theory is not suitable for modelling the thick helical spring because it always overestimates the spring compliance under a point load. A novel deflection correction factor is proposed, which

is simultaneously based on the E/B theory of slender beams and the A/G correction. Novel stress correction factors based on the von Mises equivalent stress and the Göhner correction are proposed. The new approximate correction factors seem to be valid for arbitrarily large pitch angles. The obtained correction factors are compared with detailed parametric FEM analyses and expressions from the literature. Continuum (3D) and beam (1D) FE solutions are considered in parametric numerical analyses.

The paper is structured as follows. In section 2, a theoretical framework for the helical spring is established using various correction factors from the literature. Novel spring deflection and stress correction factors are derived and discussed. In section 3, FE modelling is briefly outlined and a suitable mesh is proposed. In section 4, detailed analytical and parametric numerical analyses are performed by varying the spring index and pitch angle simultaneously. In section 5, a benchmark example is given using all previous concepts and comparing the analytical and FEM results. Section 6 gives concluding remarks. Finally, Appendix A provides all relevant results in a tabulated, compact form. The new correction equations obtained in this study may be of particular interest to potential users, *i.e.* to engineers in charge of research and development, structural analysts, and spring designers.

## 2. CYLINDRICAL COIL SPRING COMPUTATIONAL MODEL AND METHODS

In this chapter, the basic constitutive equations for the cylindrical spring under a quasi-static point load are derived. A computational model of the spring is shown in Figure 1, in two projections. Loading is denoted by the point force  $F_0$ , and the corresponding deflection in the  $z$  axis direction by  $\delta$ . Geometrical properties of the spring are the mean spring coil diameter  $D$ , spring wire diameter  $d$ , spring pitch  $l$ , and the number of active coils  $n$ . For the idealized spring model shown in Figure 1,  $n = 2$ . The circular cross-section is greyed in Figure 1b).

The boundary conditions (BCs) are hinged (reference point  $B_{RP}$ ) or moving hinged (reference point  $A_{RP}$ ). In terms of physics,  $B_{RP}$  is actually a spherical joint with additionally prohibited rotation around the  $z$  axis in order to prevent the rigid body (RB) movement [37],[38]. The same BCs are prescribed for the FEM model in section 3. The point load of constant magnitude  $F_0$  acts on the top of the spring through  $A_{RP}$ . This model is consistent with the referent models from the literature [1],[3]-[12],[16]-[18] and DIN standards [29],[35].

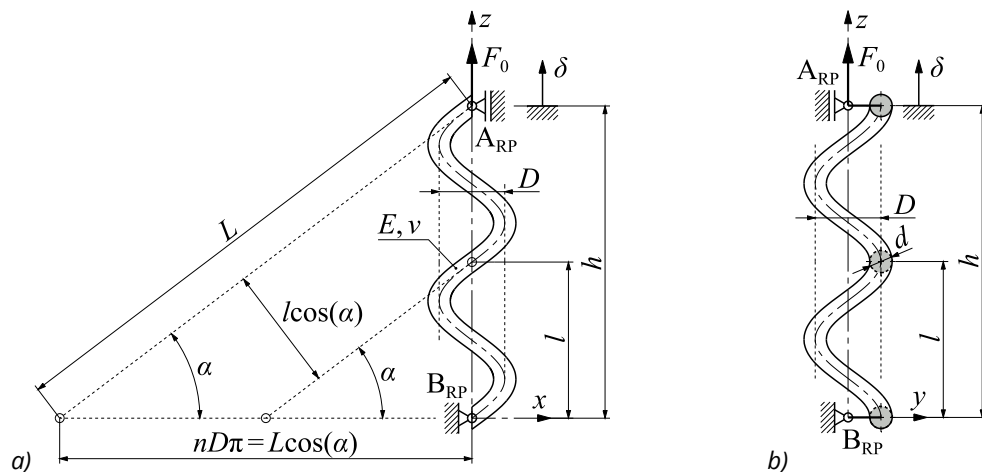


**Fig. 1** Helical coil spring model - geometric parameters and loading: a) side view, b) front view

Basic geometric relations for the spring shown in the scheme in Figure 1 are [16]-[18]:

$$h = n \cdot l, \quad \alpha = \arctan\left(\frac{l}{\pi D}\right), \quad L = \frac{nD\pi}{\cos(\alpha)} = n\sqrt{l^2 + (D\pi)^2}, \quad A = \frac{d^2\pi}{4}, \quad (1a-d)$$

where  $h$  is the spring height,  $\alpha$  is the pitch angle,  $L$  is the total length of spring wire, and  $A$  is the circular cross-section area of the spring. Using Castigliano's energy theorem [6] and fundamental SOM relations, one obtains the expressions for the nominal spring deflection  $\delta_{nom}(\alpha \rightarrow 0)$  and the nominal shear stress  $\tau_{nom}(C \gg 1)$  [16]-[18] as:

$$C = \frac{D}{d}, \quad G = \frac{E}{2(1+\nu)}, \quad M_t = F_0 \frac{D}{2} \Rightarrow \delta_{nom} = \frac{8F_0 C^3 n}{Gd}, \quad (2a-f)$$

$$\tau_{nom} = \frac{8F_0 C}{d^2 \pi}, \quad \sigma_{eqv, nom}^{HMH}(\text{pure torsion}) = \sqrt{3} \tau_{nom}$$

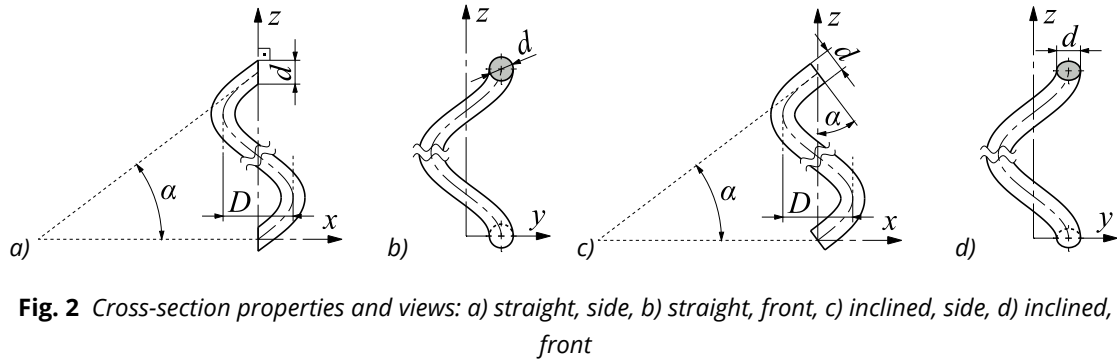
where  $C$  is the spring index [6],[7],  $G$  is the shear modulus,  $E$  is Young's modulus,  $\nu$  is Poisson's ratio, and  $M_t$  is the torsion moment with respect to the force  $F_0$  rigid arm of length  $D/2$ . Furthermore,  $\sigma_{eqv, nom}^{HMH}$  denotes the nominal von Mises (*i.e.* Huber-Mises-Hencky) distortion energy equivalent stress criterion for pure torsion [1],[3]-[8],[16]-[18].

For practical applications [9], the recommended common values of spring index are  $4 \leq C \leq 12$  [6],[10] or  $3 \leq C \leq 12$  [8]. An even narrower range of  $6 \leq C \leq 12$  can be found in [7]. At higher indices of  $C_{max} > 12$ , the spring is likely to buckle [7] or tangle [7],[10], while springs with indices of  $C_{min} < 4$  may become difficult to form/manufacture [10]. In order to thoroughly check the numerical accuracy of the expressions proposed later in the text,  $C$  values of the parametric analyses are varied outside of these recommended ranges. If the spring is thick (*i.e.* has small  $C$  values) or steep (*i.e.* has large  $\alpha$ ), the correction factors  $K$  which compensate for additional effects due to geometric deviations should be included [16]-[18]. The corrected deflection  $\delta_{cor}$  and stress  $\sigma_{cor}$  for Eqs. (2d,f) are given as:

$$\delta_{cor} = K_\delta \delta_{nom}, \quad \sigma_{eqv, cor}^{HMH} = K_\sigma \sigma_{eqv, nom}^{HMH}, \quad E_{rel, max} = \left(\frac{K_{max}}{K_{min}} - 1\right) \times 100 \%, \quad (3a-c)$$

where  $K_\delta$  is the deflection correction factor,  $K_\sigma$  is the stress correction factor and  $E_{rel, max}$  from Eq. (3c) is the maximum relative error between corresponding corrections  $K$ . The relative error  $E_{rel, max}$  is used in this study as an effective measure or indicator of the accuracy for the proposed correction factors.

Furthermore, two types of springs with respect to the inclination of the corresponding circular cross-section are considered. The geometry of a single helical spring coil (*i.e.*,  $n = 1$ ) is shown in Figure 2 for the straight and inclined cross-sections, respectively. "Straight" implies that the undeformed cross-section is parallel to the vertical spring axis  $z$ , no matter where the spring is virtually cut by a vertical plane [12],[30]. "Inclined" assumes that the undeformed cross-section is perpendicular to the spring helix tangent (see the diagonal dashed line in Figure 2c). The inclined cross-section may be approximated with the simple beam theory, due to the perpendicularity between the imposed helix tangent and the cross-section. The straight cross-section may be approximated with the beam theory only for small  $\alpha$ , while the TOE relations should be used in all other cases [1],[15],[19]. These are two extreme types of geometric constraints. However, the real final spring geometry solely depends on the type of manufacture [9]. For the front view of the inclined cross-section in Figure 2d), the area of the cross-section looks like an ellipse in this perspective.



In order to simplify the calculations made for intended engineering applications, the following limits are imposed. Springs are geometrically linear and the material is linear, homogenous, and isotropic. No residual stresses [16],[17], or original imperfections due to manufacturing [9] are taken into account.

With the goal of a more general approach and broader applicability, further results are presented in a dimensionless form as a function of three corresponding parameters: spring index  $C$ , pitch angle  $\alpha$  and Poisson's ratio  $\nu$ , i.e.  $K_{\delta,\sigma} = K_{\delta,\sigma}(C,\alpha,\nu)$ . It is important to emphasize that a closed-form solution to this type of problem is not found in the current literature. Hence, all solutions found in the literature are essentially approximate [1].

## 2.1 STRAIGHT CROSS-SECTION

The improved  $A/G$  ( $A/G,i$ ) deflection and stress corrections proposed in [18] are given by the following expressions, respectively:

$$k_{\delta,i} = 0.185 \Rightarrow K_{\delta,A/G,i} = 1 - \frac{\overbrace{3}^{C\text{-dependent}}}{16C^2} + \frac{\overbrace{3+k_{\delta,i}+\nu}^{\nu\text{-dependent}} \overbrace{\tan^2(\alpha)}^{\alpha\text{-dependent}}}{2(1+\nu)}, \quad (4a,b)$$

and

$$k_{T/W} = \frac{\overbrace{1+2\nu}^{\nu\text{-dependent}}}{2(1+\nu)} \Rightarrow K_{\sigma,A/G,i} = \overbrace{1.005}^{\text{constant}} + \frac{\overbrace{5}^{C\text{-dependent}}}{4C} + \frac{\overbrace{8}^{C\text{-dependent}}}{7C^2} + \frac{\overbrace{k_{T/W}}^{\nu\text{-dependent}} \overbrace{\tan^2(\alpha)}^{\alpha\text{-dependent}}}{\phantom{1}}. \quad (5a,b)$$

When zero pitch angle  $\alpha$  values are considered, the corrections which account for shear are governed only by the spring index  $C$ , which is marked by curly brackets in Eqs. (4,5). For higher values of  $\alpha$ , the influence of Poisson's ratio  $\nu$  becomes more dominant [18]. Hence, these two effects, i.e. spring thickness defined via spring index  $C$  and pitch angle  $\alpha$ , are approximately decoupled for straight cross-section. Correspondingly, for a small  $\alpha$ , Göhner ( $G$ ), [1],[15],[22], proposed the following  $C$ -governed/dependent stress correction:

$$K_{\sigma,G} = 1 + \frac{5}{4C} + \frac{7}{8C^2} + \frac{1}{C^3} \equiv 1 + \frac{1.25}{C} + \frac{0.875}{C^2} + \frac{1}{C^3}. \quad (6)$$

Equation (6) is also reported by the same author in [21] but without the last term  $C^{-3}$ , i.e. the third order approximation [23]. Furthermore, other variations of the Göhner stress correction may be found in the literature:

$$K_{\sigma,G,B} = \left( \frac{C}{C-1} + \frac{1}{4C} + \frac{1}{16C^2} \right) \left( \frac{C^2 - 1}{C^2 - 0.8125} \right), \quad K_{\sigma,G,T} = \frac{\frac{1}{1-C^{-1}} + \frac{1}{4C} + \frac{1}{16C^2}}{1 + \frac{3}{16(C^2 - 1)}}, \quad (7a-c)$$

$$K_{\sigma,G,B} \equiv K_{\sigma,G,T} = K_{\sigma,G,T/B}$$

Equation (7a), ( $G,B$ ), is reported in [25] and Eq. (7b), ( $G,T$ ), in [1],[15],[22] and [26]. After some mathematical simplifications, it may be noted that Eqs. (7a,b) are numerically equivalent, as implied in Eq. (7c). Moreover, the corrections by Henrici ( $H$ ) [23], and Bergsträsser ( $B$ ) [15],[25], respectively write as:

$$K_{\sigma,H} = 1 + \frac{5}{4C} + \frac{7}{8C^2} + \frac{155}{256C^3} + \frac{11\,911}{24\,576C^4} + \dots, \quad K_{\sigma,B} = \frac{4C+2}{4C-3} \equiv \frac{C+0.5}{C-0.75}. \quad (8a,b)$$

Finally, the Wahl relation ( $W,m$ ) modified with the Timoshenko/Wahl shear stress correction  $k_{T/W}$  from Eq. (5a) and Poisson's ratio  $\nu$  set to zero (as recommended in [16],[17]), yields the following simple expression:

$$K_{\sigma,W,m} = \frac{4C-1}{4C-4} + \frac{k_{T/W}(\nu=0)}{C} = \frac{4C-1}{4C-4} + \frac{1}{2C}. \quad (9)$$

Equation (9) was already implied in [16]-[18] but not explicitly proposed in the present form. It provides a less conservative prediction than the original Wahl design equation [1],[11]. This conclusion is drawn from the fact that Wahl himself noted that his correction factor was overly conservative when compared to the values obtained experimentally [1] and to the Göhner approximation, Eqs. (6,7). Using Eq. (3c), the maximum relative error between Eq. (5b) (for  $\alpha = 0$ ), and Eqs. (6-9) for a spring index of as low as  $C = 2.5$  is obtained as  $E_{rel,max} \approx 1.63\%$ . Bergsträsser, Eq. (8b), predicts the most conservative results for  $C = 2.5$ . For a spring index of  $C = 4$ , i.e.  $C = C_{min}$ ,  $E_{rel,max} \approx 1.01\%$ . For higher spring indices, i.e. for slender springs,  $E_{rel,max} \rightarrow 0$ . Thus, it can be concluded that any of the relevant relations from Eqs. (6-9), i.e.  $K_{\sigma,general}$ , may be used as a template for larger spring angles when combined/superpositioned with the right-hand side of Eq. (5b), i.e. the term  $k_{T/W} \tan^2(\alpha)$ . This is defined in the relations:

$$K_{\sigma,\alpha} = K_{\sigma,general} + k_{T/W} \tan^2(\alpha) \Rightarrow K_{\sigma,G,\alpha} = K_{\sigma,G} + k_{T/W} \tan^2(\alpha), \quad (10a,b)$$

where the Göhner solution from Eq. (6) and its modified version from Eq. (10b) are chosen for further verification in the following chapters. Equations (9,10) are considered to be minor contributions of this study.

## 2.2 INCLINED CROSS-SECTION

Inclined cross-sections represent the main theoretical framework of this study and are considered next. From Castigliano's theorem, Timoshenko [5] proposed the following expression for spring deflection:

$$I_a = \frac{d^4 \pi}{64}, \quad I_p = 2I_a = \frac{d^4 \pi}{32} \Rightarrow \delta_{C/T/G} = F_0 L \frac{D^2}{4} \left[ \frac{\overbrace{\sin^2(\alpha)}^{bending}}{I_a E} + \frac{\overbrace{\cos^2(\alpha)}^{torsion\ shear}}{I_p G} \frac{1}{\beta_G^n} \right], \quad (11a-c)$$

where  $I_a$  and  $I_p$  are the axial and polar moments of inertia, respectively. Furthermore,  $\beta_G$  is the additional shear correction:

$$\beta_G = 1 + 3 \left( \frac{1}{C} \right)^2 \left\{ 16 \left[ 1 - \left( \frac{1}{C} \right)^2 \right] \right\}^{-1} = 1 + \frac{3}{16(C^2 - 1)}, \quad (12)$$

for which Timoshenko [5] references Göhner. As stated by Yıldırım [43], the derivation of  $\beta_G$  is not explicitly given in [5]. Nevertheless, it is clear that the bending and corrected torsion shear effects are taken into account, but the axial effects are neglected in Eq. (11c). Next, from Eqs. (3a,11c), the following deflection correction factor is obtained:

$$K_{\delta,C/T/G} = \overbrace{\cos(\alpha)}^{\text{torsion}} \frac{1}{\beta_G^n} + \frac{\overbrace{\sin(\alpha)\tan(\alpha)}^{\text{bending}}}{1+\nu}, \quad (13)$$

where, by setting the power  $n$  to 1 and using Eq. (12), one obtains the following closed-form dimensionless correction:

$$n = +1 \Rightarrow K_{\delta,C/T/G} = \frac{16(C^2 - 1)\cos(\alpha)}{(16C^2 - 13)} + \frac{\sin(\alpha)\tan(\alpha)}{1+\nu}. \quad (14a,b)$$

In [16], the power  $n$  was set to  $-1$  due to the fact that Eq. (14b) underestimates the deflection when considering large angles  $\alpha$ . In a similar vein, the Göhner deflection correction from [15] writes as:

$$K_{\delta,G} = \overbrace{\cos(\alpha)}^{\text{torsion}} \frac{1}{\left[ 1 + \frac{3 \cos^4(\alpha)}{16 C^2 - 1} \right]^n} + \frac{\overbrace{2G \sin(\alpha)\tan(\alpha)}^{\text{bending}}}{E}, \quad (15)$$

where, analogously to Eq. (13), only the corrected torsion and bending effects are considered, without any axial effects. By simplifying Eq. (15) via Eq. (2b) and setting  $n$  to 1, one obtains:

$$n = +1 \Rightarrow K_{\delta,G} = \frac{\cos(\alpha)}{1 + \frac{3 \cos^4(\alpha)}{16 C^2 - 1}} + \frac{\sin(\alpha)\tan(\alpha)}{1+\nu}. \quad (16a,b)$$

Again, analogously to Eq. (14), by setting  $n$  to 1, the spring deflection is underestimated according to the results obtained in [17]. However, the small angle effects are still studied first. Thus, the zero pitch angle  $\alpha$  limit analysis is performed on Eqs. (14b) and (16b). Both relations yield the same result:

$$n = +1 \Rightarrow \lim_{\alpha \rightarrow 0} K_{\delta,G} \equiv \lim_{\alpha \rightarrow 0} K_{\delta,C/T/G} = \frac{1}{\beta_G^n} = 1 + \frac{3}{13 - 16C^2}. \quad (17a,b)$$

Furthermore, in the study by Yıldırım [43], detailed analyses of springs of different cross-sections were performed employing Castigliano's theorem [6] and the Timoshenko thick beam [45]-[50]. When considering the circular-section [43], the total tip deflection  $\delta$  of the spring may be divided into direct shear/torsion shear contributions:

$$\delta_{shear} = k_{shear}^{-1} F \pi n \frac{D \cos(\alpha)}{GA}, \quad \delta_{torsion} = F \pi n \frac{D^3 \cos(\alpha)}{4GI_p}, \quad (18a,b)$$

and the axial/bending, *i.e.* flexural, contributions:

$$\delta_{axial} = F \pi n \frac{D \sin(\alpha) \tan(\alpha)}{EA}, \quad \delta_{bending} = F \pi n \frac{D^3 \sin(\alpha) \tan(\alpha)}{4EI_a}. \quad (19a,b)$$

In Eq. (18a),  $k_{shear}$  is known as the (Timoshenko) shear correction factor [45]-[50]. The total deflection of such a thick beam/spring is obtained by the linear superposition of Eqs. (18,19), which yields:

$$\delta_{Beam,T} = \delta_{shear} + \delta_{torsion} + \delta_{axial} + \delta_{bending}, \quad (20)$$

and after inserting the corresponding geometric values from Eqs. (18,19) and simplifying, one obtains:

$$\delta_{Beam,T} = 2F_0 D n \frac{2(\nu+1)(d^2 k_{shear}^{-1} + 2D^2) \cos(\alpha) + (d^2 + 4D^2) \sin(\alpha) \tan(\alpha)}{d^4 G(1+\nu)}. \quad (21)$$

Although in somewhat different notation, Eq. (21) is originally obtained and proposed in [43]. Regarding the shear correction factor  $k_{shear}$ , the best-known corrections for circular cross-sections are Cowper's [50] and original Timoshenko's [46] corrections. These respectively write as:

$$k_{shear} = k_{Cowper} = \frac{6(1+\nu)}{7+6\nu} < 1 (\nu = 0 - 0.5),$$

$$k_{shear} = k_{Timoshenko} = \frac{6(1+\nu)^2}{7+12\nu+4\nu^2} < 1 (\nu = 0 - 0.5) \quad (22a,b)$$

In [43], the Cowper correction, Eq. (22a), was used. The accuracy of relevant shear corrections can be debated [52]. Kaneko, [48],[49], performed a comprehensive systematic analysis of various shear coefficients proposed in the literature, including Cowper's from Eq. (22a). His conclusion was that the values reported in Timoshenko's seminal paper [46], *i.e.* Eq. (22b), show the best agreement with the experimental results [49]. However, Cowper's correction seems to be still the most popular choice in the literature [16],[17],[43]. It is also readily implemented in *Abaqus* [37], which makes it convenient for further verification. From Eq. (21) and Eq. (3a), the Timoshenko-based beam/spring deflection correction is obtained in dimensionless form as:

$$K_{\delta,Beam,T} = \frac{\delta_{Beam,T}}{\delta_{nom}} = \left( \frac{torsion}{\hat{1}} + \frac{\overbrace{k_{shear}^{-1}}^{direct\ shear}}{2C^2} \right) \cos(\alpha) + \left( \frac{bending}{\hat{1}} + \frac{\overbrace{1}^{axial}}{4C^2} \right) \frac{\sin(\alpha) \tan(\alpha)}{(1+\nu)}, \quad (23)$$

where the torsion, direct shear, bending and axial contributions are outlined via curly brackets. By performing the limit analysis on Eq. (23) for small/zero pitch angles, one obtains the following simple expression:

$$K_{\delta,Beam,T/C} \equiv \lim_{\alpha \rightarrow 0} \frac{\delta_{Beam,T}(k_{shear} = k_{Cowper})}{\delta_{nom}} = 1 + \frac{k_{Cowper}^{-1}}{2C^2} = 1 + \frac{7+6\nu}{12C^2(1+\nu)}. \quad (24)$$

Equation (24) in the form given above was derived and proposed in [16], where the zero pitch angle was initially assumed. This confirms the approaches of both methods [16],[43]. It must be pointed out that an expression similar to Eq. (23) has already been reported by Dym [51]. However, instead of  $k_{Cowper}$ , the unit term was used for shear contribution, *i.e.*  $k_{shear} = k_{Dym} = 1$  [51]. Setting the shear correction to unity in Eq. (23) and performing the zero angle limit analysis, one obtains:

$$\lim_{\alpha \rightarrow 0} K_{\delta, Dym} \equiv \lim_{\alpha \rightarrow 0, k_{shear}^{-1} \rightarrow 1} K_{\delta, Beam, T} = 1 + \frac{1}{2C^2} \equiv K_{\delta, Shigley} \quad (25)$$

The same is also obtained in Shigley's textbook [6]. Since for any physical value of Poisson's ratio:

$$k_{Cowper}^{-1} > 1 \Rightarrow \frac{k_{Cowper}^{-1}}{2C^2} (\nu = 0 - 0.5) > \frac{1}{2C^2} \Rightarrow K_{\delta, Beam, T} > K_{\delta, Dym} \quad (26a-c)$$

one may expect that the Timoshenko/Cowper shear correction will produce a larger predicted spring deflection compared to the shear corrections from Eq. (25) by Dym/Shigley. However, when analysing the structure of Eq. (23), it is obvious that the direct shear and axial contributions are at least an order of magnitude lower compared to the torsion and bending contributions in the case of relatively thick springs. Furthermore, it is stated in [17] that the Timoshenko beam with the Cowper shear correction may overestimate the spring deflection. This is especially evident for small  $C$  values. Moreover, it was actually demonstrated experimentally [1] and numerically [17],[18] that thick springs may exhibit the values of deflection correction factors of less than one. This effect can be considered as a surprising and unexpected result. It is employed in the following section to obtain a new deflection correction factor.

### 2.3 DERIVATION AND RESULTS OF NOVEL DEFLECTION AND STRESS CORRECTION FACTORS FOR THE INCLINED CROSS-SECTION

In this section, novel correction factors are proposed. The loading scheme of the helical coil spring model is given in Figure 1 and its geometry in Figure 2c) and d). The deflection correction factor has been derived by linearly combining the torsion (with neglecting the direct shear), bending and axial contributions from Eq. (23) and the  $C$ -dependent improved  $A/G, i$  correction from Eq. (4) [18]. This expression now writes as:

$$K_{\delta, A/G, m} = \frac{-3}{16C^2} \cos^6(\alpha) \Rightarrow K_{\delta, Beam, A/G} = \lim_{k_{Cowper}^{-1} \rightarrow 0} K_{\delta, Beam, T} + K_{\delta, A/G, m} =$$

$$\overbrace{\cos(\alpha) + \left(1 + \frac{1}{4C^2}\right) \frac{\sin(\alpha)\tan(\alpha)}{(1+\nu)}}^{K_{\delta, Beam, E/B}} + K_{\delta, A/G, m} \quad (27a, b)$$

where  $\cos^6(\alpha)$  from Eq. (27a) is the approximate scaling factor, analogously to the Göhner shear scaling factor  $\cos^4(\alpha)$  from Eq. (15). This scaling factor is now used in order not to underestimate deflection when considering larger pitch angles  $\alpha$ . The proposed Eq. (27) is considered to be a novelty and an important contribution of this study. By setting the zero angle, Eq. (27b) reverts to:

$$\lim_{\alpha \rightarrow 0} K_{\delta, Beam, A/G} \equiv \lim_{\alpha \rightarrow 0} K_{\delta, A/G, i} = 1 - \overbrace{\frac{3}{16C^2}}^{\text{negative contribution}}, \quad (28)$$

which is the original  $A/G$  equation [12] (with the outlined *negative* correction contribution) verified in [17],[18]. By setting the term  $K_{\delta, A/G, m} = 0$  in Eq. (27b), the ordinary thin beam  $E/B$  theory correction  $K_{\delta, Beam, E/B}$  is obtained. Furthermore, by neglecting both the direct shear and axial contributions in Eq. (23), a simple relation:

$$K_{\delta, Beam, t+b} = \cos(\alpha) + \frac{\sin(\alpha)\tan(\alpha)}{(1+\nu)}, \quad (29)$$

is obtained. It may serve as a basic approximation for the realistic spring deflection correction with a large  $\alpha$ .

Next, a new stress correction factor is considered. Analogously to the deflection contributions from Eqs. (18,19), multiaxial stress contributions [6] for the inclined cross-section may be divided into the direct shear/torsion shear stress:

$$\tau_{shear(max)} = \frac{4}{3} \frac{F_0}{A} \cos(\alpha), \quad \tau_{torsion} = \frac{M_t}{I_p} \frac{d}{2} \cos(\alpha) = \tau_{nom} \cos(\alpha), \quad (30a,b)$$

and the normal stress due to the axial and the bending, *i.e.* flexural load:

$$\sigma_{axial} = \frac{F_0}{A} \sin(\alpha), \quad \sigma_{bending} = \frac{M_t}{I_a} \frac{d}{2} \sin(\alpha) = 4\sigma_{axial} C. \quad (31a,b)$$

The factor “ $4/3$ ” in Eq. (30a) denotes the actual maximum direct shear stress in the circular cross-section [6], rather than the mean shear stress. The shear and normal contributions combined from Eqs. (30,31) are linearly superimposed as:

$$\tau_{max} = \tau_{shear} + \tau_{torsion}, \quad \sigma_{max} = \sigma_{normal} = \sigma_{axial} + \sigma_{bending}. \quad (32a,b)$$

By considering the zero pitch angle  $\alpha$ , the equivalent (shear) stress correction  $K_{\sigma, Beam, T}$  for Eq. (32a) writes:

$$K_{\sigma, Beam, T}(\alpha=0) = \frac{\tau_{max}(\alpha=0)}{\tau_{nom}} = 1 + \frac{2}{3C}. \quad (33)$$

Equation (33) is in fact completely consistent with Eq. (24), *i.e.* the thick Timoshenko beam/spring with a small/negligible pitch angle. Taking into consideration all four stress contributions, the equivalent stress theory is used with the maximum distortion energy, *i.e.* the von Mises criterion [6]. However, the direct torsion shear from Eq. (30a) is omitted in favour of the slightly modified Göhner stress correction from Eq. (6). By combining Eqs. (30b), (31a,b), (32b) and (6), one obtains:

$$\sigma_{eqv, G}^{HMH} = \sqrt{\sigma_{max}^2 + 3(K_{\sigma, G, m} \tau_{torsion})^2} = 4F_0 \frac{\sqrt{[(d+4D)\sin(\alpha)]^2 + 12[K_{\sigma, G, m} D \cos(\alpha)]^2}}{d^3 \pi}. \quad (34)$$

Scaling Eq. (34) with the nominal equivalent stress from Eq. (2f) and simplifying it, one obtains the final expression for equivalent correction

$$K_{\sigma,eqv,G}^{HMH} \equiv K_{\sigma,Beam,G} = \frac{\sigma_{eqv,G}^{HMH}}{\sigma_{eqv,nom}^{HMH}} = \frac{\sqrt{\left[ \left( \overset{\text{axial}}{\hat{1}} + \overset{\text{bending}}{4C} \right) \sin(\alpha) \right]^2 + 12 \left[ \overset{\text{torsion \& shear}}{K_{\sigma,G,m}C} \cos(\alpha) \right]^2}}{2\sqrt{3}C}, \quad (35)$$

where the Göhner shear stress correction  $K_{\sigma,G,m}$  in Eqs. (34,35), modified from Eq. (6), writes as:

$$K_{\sigma,G,m} = 1 + \frac{5}{4C} + \frac{7}{8C^2} + \frac{\cos(\alpha)}{C^3}, \quad (36)$$

and  $\cos(\alpha)$  is the additional scaling factor imposed on the final polynomial coefficient  $C^{-3}$  in order not to overestimate the shear stress for larger pitch angles. This is consistent with Göhner's approximation given in [21], which completely disregards the term  $C^{-3}$ . The main flaw of the proposed Eq. (35) is that it neglects the actual change in the spring curvature when considering large pitch angles [1]. Consequently, for an increasing pitch angle  $\alpha$ , the shear stress may be slightly overestimated and the bending stress may be underestimated. Furthermore, the influence of Poisson's ratio  $\nu$  is not included in the stress correction herein due to the simple beam approximation. Despite its inherent simplifications, the combined Göhner and the regular beam-based correction factor  $K_{\sigma,Beam,G}$  from Eq. (35), is considered as the main contribution of this study. This correction factor is successfully verified in the subsequent chapters. Moreover, modifying the term  $K_{\sigma,G,m}$  in Eq. (35) by setting it to unity, the ordinary thin beam  $E/B$  theory stress correction  $K_{\sigma,Beam,E/B}$  is obtained.

For convenience and better visual representation, the proposed Eqs. (27) and (35) are shown in Figure 3a) and b), respectively, as analytical 3D surfaces. The correction factors  $K$  are denoted as functions of both the spring index  $C$  and the pitch angle  $\alpha$  simultaneously. Poisson's ratio is set to  $\nu = 0.3$  for all the cases that follow. This implies that the proposed expressions may prove to be sufficiently accurate for steel-like materials. The results for the deflection correction field  $K_\delta$  in Figure 3a) are similar to the ones presented for the straight cross-section in [18], which means that the influence of the spring index  $C$  is almost negligible compared to that of the pitch angle  $\alpha$ . However, the results for the stress correction in Figure 3b) show that there is an inconsistent sensitivity of the correction factor  $K_\sigma$  to the spring index  $C$  in combination with an increasing pitch angle  $\alpha$ . Beyond a certain value of  $C$  (*i.e.* very slender spring), the stress correction value increases for an increasing  $\alpha$ , and below a certain small value of  $C$  (*i.e.* very thick spring), the stress correction value decreases for an increasing  $\alpha$ . Hence, two important points are considered next.

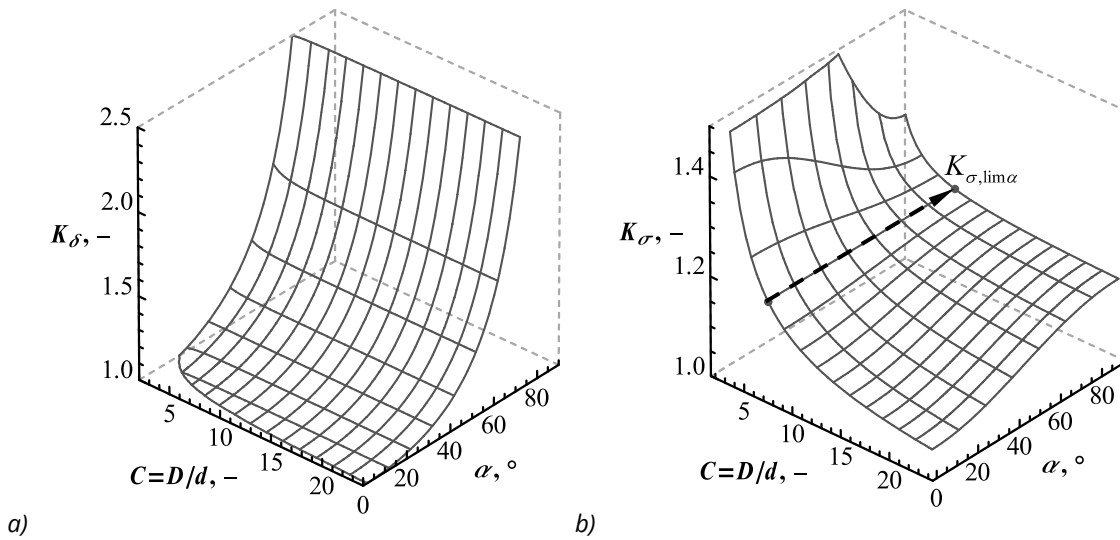


**Fig. 3** Comparison of correction factors by varying  $C(2 - 24)$  and  $\alpha(0 - 90^\circ)$ ,  $\nu = 0.3$ :

a)  $K_{\delta, Beam, A/G}(C, \alpha)$ , b)  $K_{\sigma, Beam, G}(C, \alpha)$

Firstly, one may observe that even for very large pitch angles, the stress correction  $K_\sigma$  tends to finite values, independently of the index  $C$ . It may be shown that these values actually converge to the straight bar under the simultaneous action of the axial/normal force and the bending moment for the limit value of pitch angle (*i.e.*  $\alpha \rightarrow \pi/2$ ). This is given by the following relation:

$$Beam\ limit = K_{\sigma, lim} = \lim_{\alpha \rightarrow \pi/2} K_{\sigma, eqv, G}^{HMH} = \frac{1 + 4C}{2\sqrt{3C}}. \quad (37)$$

In that case, the deflection correction  $K_\delta$  tends to infinity since the spring becomes infinitely compliant. This is shown in the singularity in Figure 3a) for values of  $\alpha > \sim 70^\circ$ . Secondly, one may see an approximately straight line/arrow in Figure 3b) for a certain value of the spring index  $C = C_{lim}$ . This value can be obtained analytically by equalling Eq. (35) with  $\alpha \rightarrow 0$  and the limit value from Eq. (37). The stress correction  $K_{\sigma, lim \alpha}$  for  $C_{lim}$  from Figure 3b) can then be obtained by inserting the solution obtained for  $C_{lim}$  into Eq. (37). The approximate values are:

$$\begin{aligned} C_{lim} (K_{\sigma, Beam, G}(\alpha \rightarrow 0) = K_{\sigma, lim}) &\cong 7.133955 \Rightarrow \\ \Rightarrow K_{\sigma, Beam, G}(C = C_{lim}) = K_{\sigma, lim \alpha} &\cong 1.19517 \end{aligned} \quad (38a, b)$$

It may be noted that the value of  $C_{lim}$  is between the constrained values,  $4 < C_{lim} < 12$ . This may be useful for spring design purposes [9],[10], as the stress correction factor  $K_\sigma$  and the corresponding stress remain approximately constant, independently of angle  $\alpha$ . This is verified in the following chapters via FEM.

Additionally, it might be insightful to point out that the numerator of Eq. (7b) is in fact a truncated approximation of the original Göhner infinite series expression [15],[22] which writes as:

$$\begin{aligned} K_{\sigma, G, T}^{numerator} &= \frac{1}{1 - C^{-1}} + \sum_{n=1}^{n_{max} \rightarrow \infty} \frac{1}{2^{2^n}} (C^{-1})^n = \\ &= \frac{1}{1 - C^{-1}} + \frac{1}{4C} + \frac{1}{16C^2} + \frac{1}{256C^3} + \frac{1}{65\ 536C^4} + \dots \approx \frac{1}{1 - C^{-1}} + \frac{1}{4C} + \frac{1}{16C^2} \end{aligned} \quad (39)$$

and that Eq. (6) is actually a modified Taylor series approximation of the simplified, *i.e.* truncated, Eq. (7). The true expression for the Taylor series expansion of Eq. (7) may be written as:

$$K_{\sigma,G}^{Taylor} = 1 + \frac{5}{4C} + \frac{7}{8C^2} + \frac{49}{64C^3} + \frac{83}{128C^4} + \frac{637}{1\,024C^5} + \frac{1\,079}{2\,048C^6} + \dots \approx 1 + \frac{5}{4C} + \frac{7}{8C^2} + \frac{1}{C^3} \cdot \quad (40)$$

It can be observed that the left-hand side polynomial of Eq. (40) most notably differs from approximate Eq. (6), *i.e.* the right-hand side of Eq. (40). The difference is in the term  $C^{-3}$  which was probably conceived by Göhner in order to compensate for higher power terms of  $C$  slightly conservatively. Nevertheless, in parametric analyses, it is observed that the differences between all Göhner's approximations considered are negligible from an engineering point of view. Considering Eqs. (6,7,39,40),  $E_{rel,max(G)}$  is less than 0.7 %, for the extremely low spring index  $C$  of 2.5.

### 3. FINITE ELEMENT MODELLING

A brief overview of FEM modelling is given in this chapter. In order to obtain non-biased numerical results, two FEM software packages with alternate solvers are used for verification: *Abaqus* [37] and *Catia* [38]. *Catia* is used as a primary verification tool because of its powerful modelling capabilities and the ability to perform a large number of iterative computations. In that sense, a completely parametric hexahedral mesh is used, with every node of the mesh defined by the user. Figure 4a)-c) show three types of cross-section meshes used.

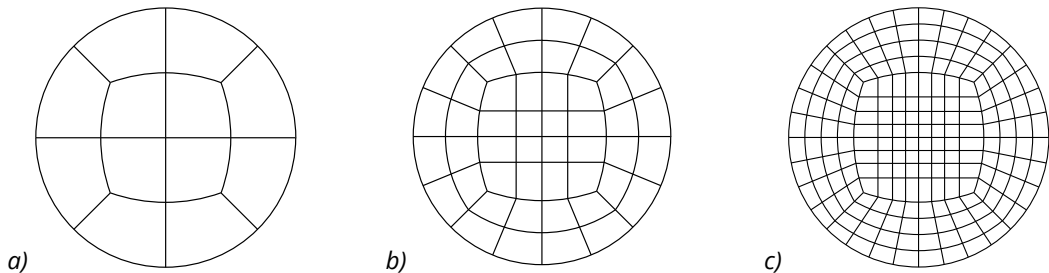


**Fig. 4** Parametric structured cross-section meshes: a) coarse, b) reference [17],[18], c) converged

The coarse mesh in Figure 4a) is used only for preliminary calculations. The reference mesh in Figure 4b) refers to the recommended parameters obtained from [17],[18], where 48 second order FEs were used per spring wire cross-section. In Figure 4c), the converged mesh denotes a very fine, detailed mesh used in this study to obtain as accurate numerical results as possible. In this mesh, 192 second order FEs are prescribed per spring cross-section. Equivalent converged meshes are used in *Abaqus* and *Catia*. Figure 5 shows the spring loading scheme with a corresponding free-body diagram and equivalent loading for the straight and inclined cross-sections, respectively. The spring tangent " $t$ " is outlined in Figure 5c) (straight cross-section) and Figure 5d) (inclined cross-section). The numerical kinematic coupling scheme from Figure 5a) is consistent with the scheme in Figure 1b) where a rigid interface, *i.e.* the rigid arm of length  $D/2$ , is defined between referent points  $A_{RP}$  and  $B_{RP}$ , and their corresponding coupling surfaces ( $A_{surface}$ ). This type of kinematic connection enables free deformation of coupling surfaces by imposing weighting factors [37]. It is labelled as "Distributing" in *Abaqus* [37] and "Smooth Spider" in *Catia* [38]. More details about the kinematic coupling and the corresponding computational model are given in [17],[18]. In Figure 5a), the location of

maximum equivalent stress is marked. The equivalent torsion moment  $M_t$  from Eq. (2c) is denoted in Figure 4b)-d). The mean spring coil diameter  $D$  is set to  $50\text{ mm}$  for all FEM analyses [16]-[18], while  $d$  and  $\alpha$ , Eq. (1b), are incrementally varied.

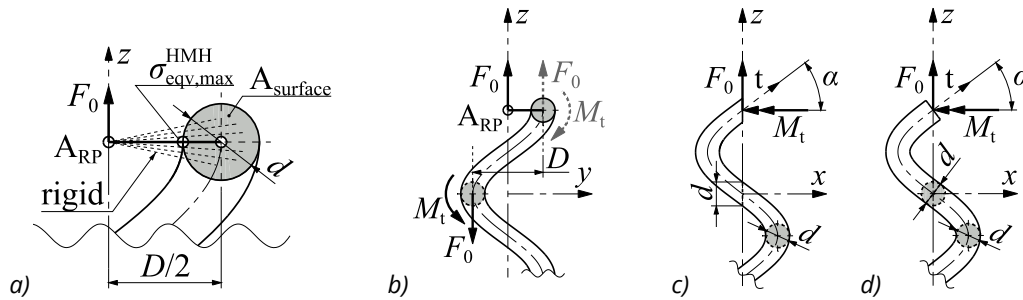


Fig. 5 Spring loading scheme: a) kinematic coupling, b) free-body diagram, c) straight, d) inclined

In both software packages, the 3D continuum second order hexahedral elements (*C3D20R* in *Abaqus*; *HE20* in *Catia*) and the beam-based first order elements (Timoshenko-based *B31* and *E/B* based *B33* in *Abaqus*; custom generalized *Beam* elements in *Catia*) are used for parametric computations which are performed next.

#### 4. PARAMETRIC ANALYSIS

In this chapter, the theoretical framework from section 2 and the FE modelling from section 3 are unified. First, the zero pitch spring angle is considered for one isolated coil, where  $n = 1$ . The computational spring model then deteriorates to a complete, sliced torus with BCs prescribed according to Figure 1. The normalized results with the coarse mesh are shown in Figure 6. The high stress gradient on the inner side of the spring coil is observed in Figure 6c).

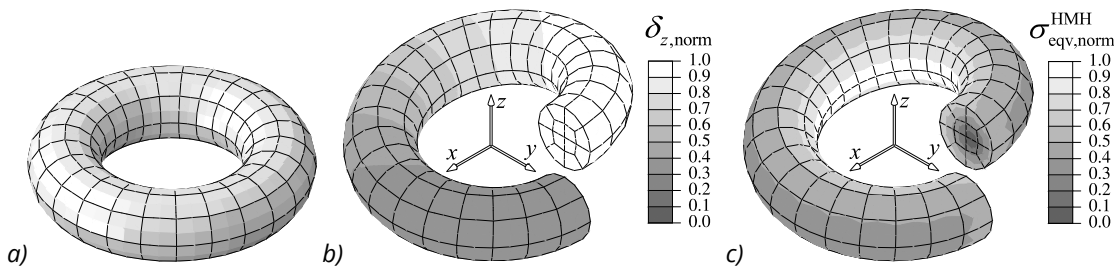


Fig. 6 FEM spring model, coarse mesh,  $\alpha = 0^\circ$ : a) undeformed, b) norm. deflection field, c) norm. stress field

Although zero pitch angles cannot be realized in practice because of the interference between the coils, this may be an insightful benchmark for the assessment of basic deflection and stress correction factors [15]. For example, Wahl performed experimental measurements for only one half of a thick, zero pitch angle spring in his pioneering book [1]. He acknowledged that the deflection correction then tends to values of less than unity. This is consistent with Eqs. (17) and (28) and the numerical/theoretical results from [17],[18].

For the deflection correction, the following relations are benchmarked against the FEM results: Eq. (4b) (limit  $A/G, i$  with  $\alpha = 0$ ), Eq. (17b) (limit  $C/T/G$ ), Eq. (24) (*Beam, T/C*) and Eq. (25) (*Dym*, i.e. the *Dym/Shigley* limit). These are shown in Figure 7a) with the corresponding FEM results. In *Catia*, the user-defined beam FEs are employed (in legend shown as *Cat, Dym*) with the

custom unit shear correction which corresponds to  $k_{Dym} = 1$  [51]. The E/B-based beam (*Beam,E/B*) readily obtains the correction as unity, independently of the spring index  $C$ . All FEM results are scaled according to Eqs. (3a,b). For the stress correction, the following relations are tested: Eq. (5b) ( $A/G,i$  with  $\alpha = 0$ ), Eq. (6) ( $G$ , i.e. Göhner), Eq. (9) ( $W,m$ ) and Eq. (33) (Timoshenko *Beam,T*). The analytical and numerical stress correction results are shown parallelly in Figure 7b). Moreover, Figure 7a) and b) may be considered as slices of Figure 3a) and b) respectively, obtained by setting  $\alpha$  to zero.

In Figure 7a), very good agreement between the corresponding theories may be observed. However, a significant discrepancy between the concurrent SOM and TOE can be noted. For the corresponding thick shear beam-based theories, relative differences are almost non-existent. The Cowper shear correction expectedly produces a larger correction when compared to the unit shear Dym approximation. For the TOE-based assumptions and corresponding continuum FEM solutions, a “less than unity” trend is generally observed. This is especially true for smaller spring indices. It is also evident that discrepancies, i.e.  $E_{rel,max}$ , between the concurrent thick beam and TOE solutions become more prominent for small spring indices, i.e. when  $C \rightarrow 1$ . Then, the limit  $C/T/G$  solution from Eq. (17b) also underestimates both the  $A/G,i$  correction, and FEM. In Figure 7b), a rather good agreement between the corresponding stress correction theories is observed. It may be reported that the analytical Eq. (33) and the numerical Timoshenko beam shear stress constantly underestimate the TOE and continuum FE solutions. In fact, the Timoshenko beam stress correction is slightly below half of the TOE-based solutions. Interestingly, the tested Eqs. (5b,6,9) (i.e.  $A/G,i$ ,  $G$ , and  $W,m$  respectively), are all in good agreement with each other and the concurrent *Abaqus* and *Catia* FEM solutions. This proves the improved accuracy of the proposed modified Wahl formula, Eq. (9).

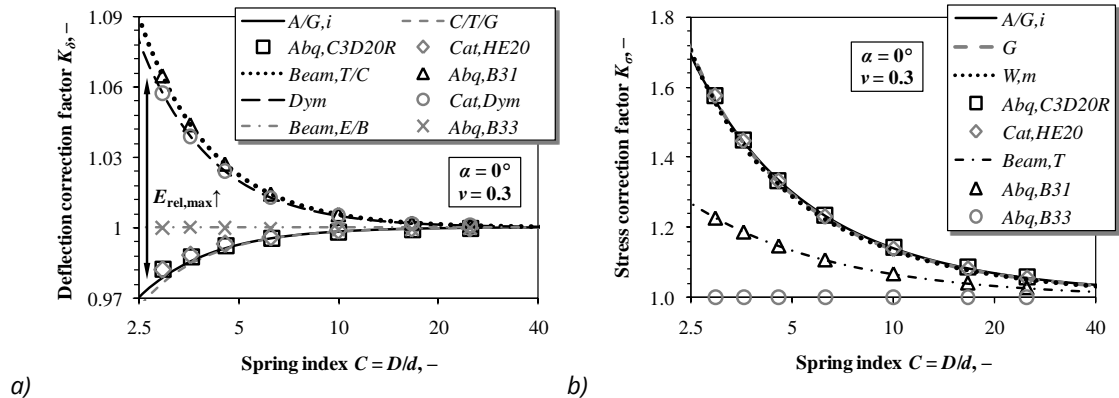


**Fig. 7** Comparison between the analytical and numerical correction factors,  $\alpha = 0^\circ$ ,  $\nu = 0.3$ : a)  $K_\delta(C)$ , b)  $K_\sigma(C)$

Next, large pitch angles are analysed. The results are presented in Figure 8-Figure 10, which may be considered as separate slices of Figure 3, obtained by fixing  $C$  and by varying  $\alpha$ . Three  $C$  values are denoted:  $C = 50/2$  (thin/slender spring, Figure 8),  $C \approx 50/\sim 7.01 \approx 7.134$  from Eq. (38a) (medium thickness spring with the limit index value  $C_{lim}$ , Figure 9), and  $C = 50/17$  (thick spring, Figure 10). The values of  $\alpha$  in Figure 8 are deliberately cut beyond  $40^\circ$  due to exceptionally long FEM computational times for larger pitch angles. Generally, very good agreement is observed in all theories, with  $E_{rel,max} < 2.5\%$  for all corresponding discrete results from Figure 8-Figure 10. In the *Catia* HE20 mesh, the index “I” stands for “inclined”. One can note the convergence of the inclined cross-section analytical and numerical stress correction factors toward  $K_{\sigma,lim}$  from Eq. (37). It may be observed that the straight cross-section predicts

much larger deflection and stress correction factors compared to the inclined cross-section. This holds true regardless of the spring index  $C$  value and can be noted in Figure 8-Figure 10. Differences between the straight and the inclined cross-section become more notable for rising values of the pitch angle  $\alpha$ . This confirms the need for considering separately the straight and the inclined cross-section of the spring. A satisfying match-up of the simple deflection correction approximation  $Beam,t+b$  from Eq. (29) with  $Beam,A/G$ ,  $Cat,HE20,I$ ,  $Beam,E/B$ , and  $Abq,B33$  results, is noted in Figure 8a), Figure 9a) and Figure 10a).

When taking into account the straight cross-section, previously proposed stress correction factor  $A/G,i$  [18] from Eq. (5), and newly proposed Göhner-based stress correction factor  $G,\alpha$  from Eq. (10b) agree very well mutually and with FEM alike. This is readily observed in Figure 8b), Figure 9b) and Figure 10b) respectively, where  $A/G,i$  is denoted via solid line, and  $G,\alpha$  is denoted via a dotted line.

For the value of  $C = 50/2 > C_{lim}$  in Figure 8b), the straight cross-section stress correction factors tend to their limit value  $K_{\sigma,lim}$  from the lower side. This holds true for both the SOM ( $Beam,E/B$ ) and TOE-based solutions. For such a slender spring, the proposed inclined Göhner-based stress correction factor ( $Beam,G$ ) from Eq. (35) slightly underestimates the stress obtained by FEM. However, practical engineering differences are negligible with the relative error being  $E_{rel,max} < 1\%$ .

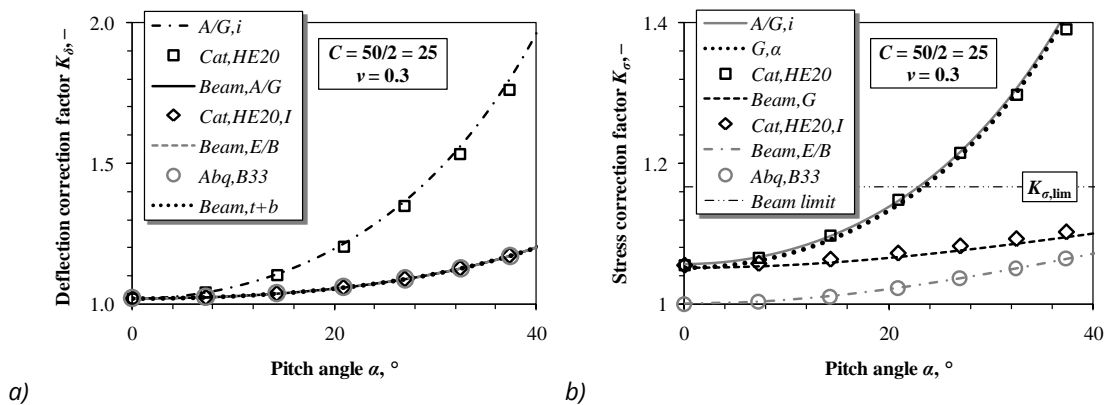


Fig. 8 Comparison between the analytical and numerical correction factors,  $C = 50/2$ ,  $\nu = 0.3$ :

a)  $K_{\delta}(\alpha)$ , b)  $K_{\sigma}(\alpha)$

A similar increasing trend in the deflection correction factor from Figure 8a) may be observed in Figure 9a). The straight cross-section provides a much larger deflection correction compared to the inclined one. The validity and accuracy of the proposed limit, *i.e.* Eq. (38), for  $K_{\sigma,lim}$  is shown in Figure 9b). It may be noted that the approximately straight line ( $Beam,G$ ) from the 3D surface plot in Figure 3b) is successfully reproduced via FEM. Moreover, the  $E/B$  beam-based stress correction again converges to beam limit value  $K_{\sigma,lim}$  from the lower side, and (expectedly) always provides non-conservative results.

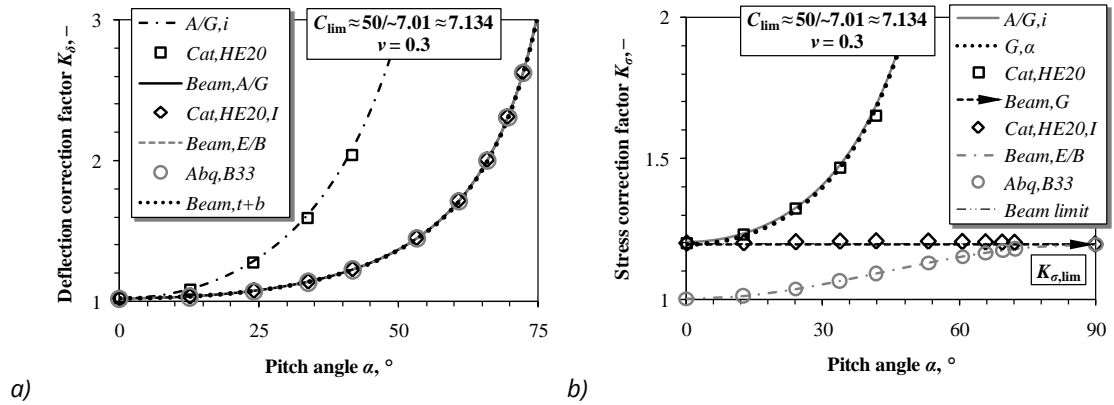


Fig. 9 Comparison between the analytical and numerical correction factors,  $C \approx 50/-7.01$ ,  $\nu = 0.3$ :  
a)  $K_\delta(\alpha)$ , b)  $K_\sigma(\alpha)$

The results shown in Figure 10 give further proof of the correctness of the proposed relations. It is interesting to see in Figure 10a) that the simple approximation from Eq. (29), i.e. *Beam,t+b*, can still capture rather accurately even the thick spring effects using only the *E/B* slender beam torsion and bending contributions. Furthermore, observing concurrently the inclined *Beam,G* and simple *Beam,E/B*-based stress correction results in Figure 10b), almost a mirror-like reflection response with respect to the  $K_{\sigma,lim}$  dash-dot-dot line is noted. Both theories converge to similar values when  $\alpha \rightarrow 90^\circ$ . However, they come from the opposite sides when  $\alpha \rightarrow 0^\circ$ . This may be of importance for the design process of large pitch angle springs since the *E/B* beam theory always underestimates the realistic/true spring stress.

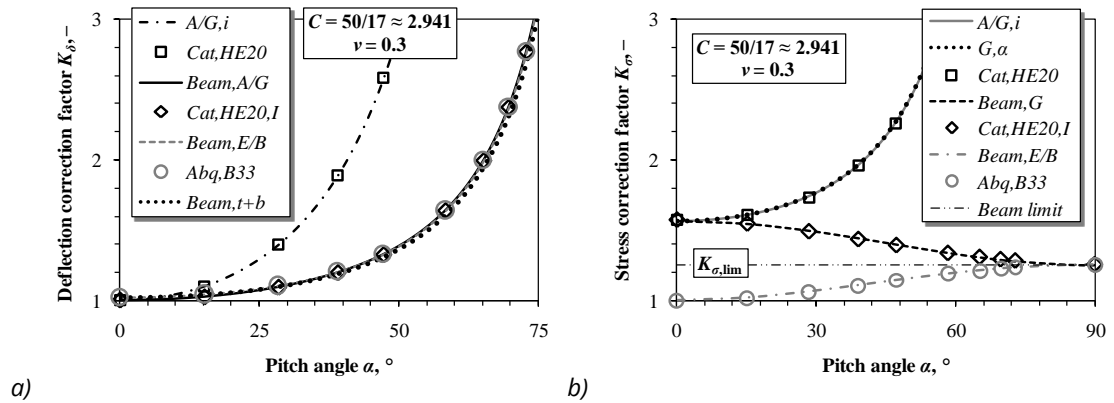


Fig. 10 Comparison between the analytical and numerical correction factors,  $C = 50/17$ ,  $\nu = 0.3$ :  
a)  $K_\delta(\alpha)$ , b)  $K_\sigma(\alpha)$

This concludes the parametric analysis section. An illustrative benchmark example is presented next.

## 5. BENCHMARK EXAMPLE

Geometric and material properties of the exemplary benchmark helical spring with a circular cross-section of diameter  $d$  are given in Table 1. The straight and inclined cross-sections are considered with the same set of spring parameters.

**Table 1** Geometric and material parameters of the benchmark helical spring

$D, mm$	$d, mm$	$n, -$	$l, mm$	$E, GPa$	$\nu, -$
50	17	1	$10 \cdot d$	200	0.3

Geometric parameters are chosen in such a way as to produce a challenging benchmark model. The obtained parameter  $C \approx 2.941$  implies a very small spring index and  $\alpha \approx 47.262^\circ$  provides an extremely large pitch angle. A coarse FE mesh is shown in Figure 11 for the purpose of adequate visual resolution. Nevertheless, the converged fine/dense mesh, analogously to Figure 4c), is used in the subsequent 3D FEM calculations. The number of nodes for the 3D and the 1D FE mesh is 230000 and 1 000, respectively. This model is fully consistent with the scheme shown in Figure 2, where Figure 11a) and b) correspond to Figure 2a) and b), while Figure 11c) and d) correspond to Figure 2c) and d). The constant quasi-static force  $F_0$  of an arbitrary magnitude is applied to the reference point  $A_{RP}$ , with regard to the schematic from Figure 1 and Figure 5a). The results obtained are tabulated in a consistent dimensionless form with respect to Eqs. (3a,b).

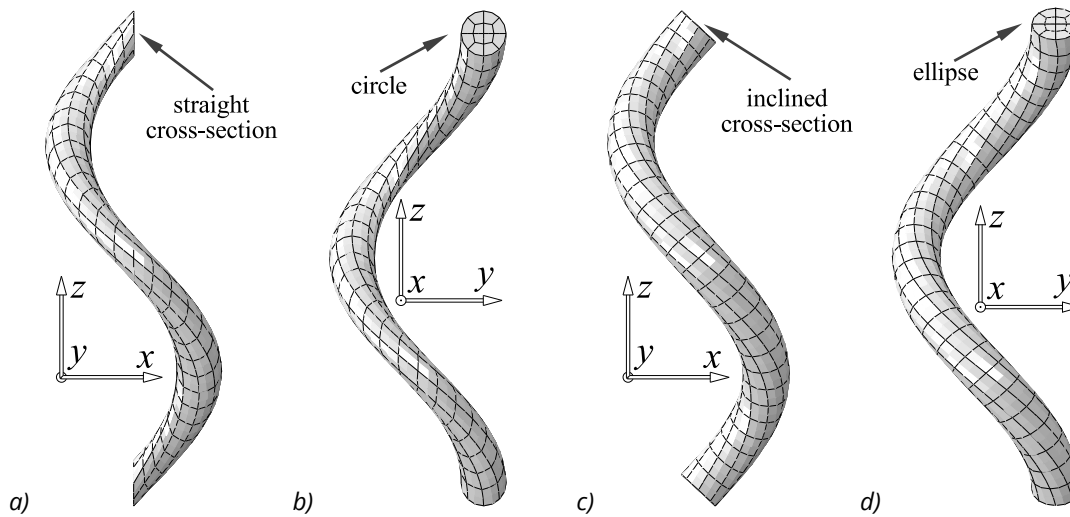


**Fig. 11** Benchmark example FE mesh views: a) straight, side, b) straight, front, c) inclined, side, d) inclined, front

Table 2 shows the results for the straight cross-section shown in Figure 11a) and b). The reported results verify the proposed correction factors from [18] and give us confidence in the correct setup of the *Catia* and *Abaqus* FEM models. Moreover, Eqs. (6-9) and the newly proposed Eq. (10) are thus successfully verified. For this particular case, the straight stress correction factors  $A/G,i$  and  $G,\alpha$  are slightly more conservative compared to FEM.

**Table 2** Benchmark example analytical and numerical correction factors, straight (TOE)

Corr.		$A/G,i$	$G,\alpha$	<i>Cat,HE20</i>	<i>Abq,C3D20R</i>	$E_{rel,max}, \%$
$K_\delta, -$	straight	2.548281	-	2.563884	2.561557	0.612
$K_\sigma, -$	straight	2.282898	2.286237	2.263492	2.259797	1.170

The inclined cross-section from Figure 11c) and d) is considered next. Table 3 shows the results for the  $E/B$  beam-based theory. Very good agreement of all corresponding solutions is observed. Even the simple beam theory *Beam,t+b* from Eq. (29) with only the torsion and bending contributions assumed gives only  $a \sim 1.4\% E_{rel,max}$ . For the *Catia* beam (*Cat,Beam,E/B*), a generalized custom cross-section is defined. It mimics the  $E/B$  slender beam cross-section

without considering Timoshenko correction for deflection due to shear,  $k_{shear}$ . Consequently, it cannot predict stress field results due to the FEM model limitations [38].

**Table 3** Benchmark example analytical and numerical correction factors, inclined (SOM beam theory)

Corr.	<i>inclined</i>	Beam,E/B	Abq,B33	Cat,Beam,E/B	Beam,t+b	$E_{rel,max}, \%$
$K_\delta$ -		1.307761	1.307759	1.307751	1.290090	1.370
$K_\sigma$ -		1.143365	1.143370	-	-	0.000

Table 4 shows the TOE-based solutions for the inclined cross-section tested in comparison with the 3D FEM solutions. Considering the limitations imposed in the simple expressions from Eqs. (27) and (35) proposed here, the results obtained may be considered highly successful. Moreover, the SOM beam-based deflection corrections  $K_\delta$  from Table 3 agree with the TOE-based corrections from Table 4 surprisingly well.

Hence, beam-based deflection correction which only considers the pitch angle  $\alpha$  (and completely disregards the spring index  $C$ ) may be sufficiently accurate when considering inclined cross-section. However, by comparing  $K_\delta \approx 2.5$  from Table 2 (straight cross-section), to  $K_\delta \approx 1.3$  from Table 3 and Table 4 respectively (inclined cross-section), the necessity for clear distinction between inclined and straight cross-sections is evident.

**Table 4** Benchmark example analytical and numerical correction factors, inclined (TOE)

Corr.	<i>inclined</i>	Beam,G	Beam,A/G	Cat,HE20,I	Abq,C3D20R,I	$E_{rel,max}, \%$
$K_\delta$ -		-	1.305644	1.308898	1.305305	0.275
$K_\sigma$ -		1.399018	-	1.391662	1.391470	0.542

The authors believe that this benchmark example provides sufficiently accurate results for all cases considered, based on the theories assumed for deriving the governing constitutive relations. Thus, the presented benchmark may be used as a fair test for numerical methods to be developed in the future, both those considering the beam-based FEs and the continuum FEs. However, the advantage of the proposed, simplified, but time-saving analytical relations must be emphasized when compared to arguably more accurate [41] but computationally much more intensive FEM. Finally, the formulae obtained herein seem to be sufficiently accurate to be included in the spring optimization algorithms [24], vibration fatigue failure assessments [16]-[18], and linear buckling/stability estimations [1],[6],[20],[44].

## 6. CONCLUSIONS

The present study deals with the estimation of deflection and multiaxial stress in the thick and steep cylindrical coil spring with a circular cross-section under axial quasi-static point load. Two distinct types of spring are discussed: the spring with a straight cross-section (if cut by a vertical plane, the cross-section is assumed to remain circular) and the spring with an inclined cross-section (it is perpendicular to the spring helix curve tangent). Analytical methods, based on the theory of elasticity and the strength of materials, are used in conjunction with the finite element method in order to study the deflection and stress of both spring types in detail.

Based on the conducted investigation, the following contributions and conclusions are emphasized:

- A basic modification to the standard Wahl stress correction is proposed in Eq. (9). This makes the Wahl stress correction factor less conservative but noticeably more accurate.

- A novel stress correction for the straight cross-section is proposed in Eq. (10b). It is based on the modified Göhner correction. It can capture large pitch angle effects in conjunction with small indices.
- A novel deflection correction factor for the inclined cross-section is proposed in Eq. (27). It is based on the Euler-Bernoulli slender beam theory and the modified Ancker and Goodier shear deflection correction.
- A novel stress correction factor for the inclined cross-section is proposed in Eq. (35). It is based on the von Mises distortion energy criterion and the modified Göhner correction for shear stress.
- The Timoshenko-based thick/short beam theory may overestimate the helical spring compliance/deflection and underestimate stress in thick springs. Hence, it is recommended to omit the Timoshenko shear correction when estimating the deflection of thick springs.
- The straight cross-section always provides higher stress and higher compliancy compared to the inclined cross-section. This is especially evident when considering larger pitch angles. In conclusion, straight and inclined cross-sections should be always analysed independently.

All of the proposed correction factors seem to be able to capture the effects of thick springs with large pitch angle simultaneously. The results obtained here are verified via a comprehensive parametric finite element analysis. The authors believe that the proposed correction factors are sufficiently accurate and relatively simple. This makes them suitable for standard engineering applications/hand calculations and may be of particular interest to spring designers, analysts, or engineers without access to commercial finite element software packages.

## 7. ACKNOWLEDGMENTS

The authors would like to express their deep appreciation to Professor Kaneko for his support, valuable suggestions, and insightful remarks during the final stages of this research work. This especially concerns observations and thoughts about the Timoshenko shear corrections and the Taylor series Göhner approximations from Eqs. (39,40).

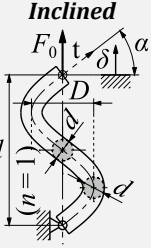
## 8. APPENDIX A: SUMMARY OF PROPOSED DEFLECTION AND STRESS CORRECTION FACTORS

Relations relevant for this study are given in the condensed form in Table A1.

The proposed relations can be used in their presented state as explicit closed-form solutions without additional numerical manipulation. By setting  $K_{\delta,A/G,m}$  for the inclined spring cross-section to zero, the corresponding deflection correction  $K_{\delta,Beam,A/G}$  reverts to the slender beam theory correction  $K_{\delta,Beam,E/B}$  with the negative direct shear deflection contribution omitted. This may slightly overestimate the spring compliancy. By setting  $K_{\sigma,G,m}$  for the inclined spring cross-section to unity, the corresponding stress correction  $K_{\sigma,Beam,G}$  deteriorates to the slender beam theory correction  $K_{\sigma,Beam,E/B}$  with the direct shear stress contribution omitted. Such an oversimplified model may significantly underestimate the realistic spring stress.

Moreover, Göhner's modified stress correction factor  $K_{\sigma,G,\alpha}$  for the straight cross-section may be a more viable expression compared to the stress correction factor  $K_{\sigma,A/G,i}$  proposed in [18] and given in Table A1, as it tends to unity when the spring index  $C$  tends to infinity. For the zero pitch angle  $\alpha$ , all corresponding correction factors provide almost equal results, no matter whether the straight or the inclined assumption is used. Thus, the consistency of results is ensured.

**Table A1** Proposed expressions for the deflection correction factors  $K_\delta$  and the stress correction factors  $K_\sigma$

	Correction factor	Note
<b>Cross-section</b>	$C = \frac{D}{d}, \quad G = \frac{E}{2(1+\nu)}, \quad \alpha = \arctan\left(\frac{l}{\pi D}\right), \quad h = n \cdot l$	$\sigma_{eqv,nom}^{HMH}(\text{pure torsion}) = \sqrt{3}\tau_{nom}$
	$\delta_{nom} = \frac{8F_0 C^3 n}{Gd}, \quad \tau_{nom} = \frac{8F_0 C}{d^2 \pi} \Rightarrow \delta_{cor} = K_\delta \delta_{nom}, \quad \sigma_{eqv,cor}^{HMH} = K_\sigma \sigma_{eqv,nom}^{HMH}$	
<b>Straight</b> 	$K_{\delta,A/G,i} = 1 - \frac{3}{16C^2} + \frac{3+k_{\delta,i}+\nu}{2(1+\nu)} \tan^2(\alpha)$	$k_{\delta,i} = 0.185$
	$K_{\sigma,A/G,i} = 1.005 + \frac{5}{4C} + \frac{8}{7C^2} + k_{T/W} \tan^2(\alpha)$	$k_{T/W} = \frac{1+2\nu}{2(1+\nu)}$
	$K_{\sigma,G,\alpha} = 1 + \frac{5}{4C} + \frac{7}{8C^2} + \frac{1}{C^3} + k_{T/W} \tan^2(\alpha)$	
<b>Inclined</b> 	$K_{\delta,Beam,A/G} = \cos(\alpha) + \left(1 + \frac{1}{4C^2}\right) \frac{\sin(\alpha)\tan(\alpha)}{(1+\nu)} + K_{\delta,A/G,m}$	$K_{\delta,A/G,m} = \frac{-3}{16C^2} \cos^6(\alpha)$
	$K_{\sigma,Beam,G} = \frac{\sqrt{[(1+4C)\sin(\alpha)]^2 + 12[K_{\sigma,G,m}C\cos(\alpha)]^2}}{2\sqrt{3}C}$	$K_{\sigma,G,m} = 1 + \frac{5}{4C} + \frac{7}{8C^2} + \frac{\cos(\alpha)}{C^3}$

## CONFLICT OF INTEREST STATEMENT

On behalf of all authors, the corresponding author states that there is no conflict of interest.

## 9. REFERENCES

- [1] A.M. Wahl, *Mechanical Springs*, First Edition, Penton Publishing Company, Cleveland, Ohio, 1944.
- [2] Y. Qiu, Y. Zhu, Z. Luo, Y. Gao, Y. Li, The analysis and design of nonlinear vibration isolators under both displacement and force excitations, *Archive of Applied Mechanics*, 2021. <https://doi.org/10.1007/s00419-020-01875-0>
- [3] W.C. Young, R.G. Budynas, A.M. Sadegh, *Roark's Formulas for Stress and Strain*, Eighth Edition, McGraw Hill, New York, 2012.
- [4] S.P. Timoshenko, *Strength of Materials, Part I, Elementary Theory and Problems*, Second Edition, D. Van Nostrand. Company, Inc., New York 1940.
- [5] S.P. Timoshenko, *Strength of Materials, Part II, Advanced Theory and Problems*, Second Edition, D. Van Nostrand. Company, Inc., New York 1940.

- [6] R.G. Budynas, J.K. Nisbett, *Shigley's Mechanical Engineering Design*, 10<sup>th</sup> Edition, McGraw-Hill, New York, 2015.
- [7] A.C. Ugural, *Mechanical Design of Machine Components*, Second Edition, CRC Press, Boca Raton 2015. <https://doi.org/10.1201/b18000>
- [8] R.C. Juvinall, K.M. Marshek, *Fundamentals of Machine Component Design*, Fifth Edition, John Wiley & Sons, Inc., Hoboken, New Jersey, 2012.
- [9] H. Carlson, *Spring Designer's Handbook*, Marcel Dekker Inc., New York and Basel, 1978.
- [10] Associated Spring Corporation, *Design Handbook: Engineering Guide to Spring Design*, Associated Spring Barnes Group, Bristol, CT, 1987.
- [11] A.M. Wahl, Helical Compression and Tension Springs, ASME Paper A-38, *Journal of Applied Mechanics* 2(1) (1935) A-35–A-37. <https://doi.org/10.1115/1.4008599>
- [12] C.J.Jr. Ancker, J.N. Goodier, Pitch and Curvature Correction for Helical Springs, *Journal of Applied Mechanics, Transactions of the ASME* 25(4) (1958) 466–470. <https://doi.org/10.1115/1.4011859>
- [13] L. Del Llano-Vizcaya, C. Rubio-González, G. Mesmacque, T. Cervantes-Hernandez, Multiaxial fatigue and failure analysis of helical compression springs, *Engineering Failure Analysis* 13(8) (2006) 1303–1313. <https://doi.org/10.1016/j.engfailanal.2005.10.011>
- [14] Y. Prawoto, M. Ikeda, S.K. Manville, A. Nishikawa, Design and failure modes of automotive suspension springs, *Engineering Failure Analysis* 15(8) (2008) 1155–1174. <https://doi.org/10.1016/j.engfailanal.2007.11.003>
- [15] Research Committee on the Analysis of Helical Spring, *Report of Research Committee on the Analysis of Helical Spring, Transactions of Japan Society of Spring Engineers* 2004(49) (2004) 35–75. <https://doi.org/10.5346/trbane.2004.35>
- [16] D. Čakmak, H. Wolf, Ž. Božić, M. Jokić, Optimization of an inerter-based vibration isolation system and helical spring fatigue life assessment, *Archive of Applied Mechanics* 89(5) (2019) 859–872. <https://doi.org/10.1007/s00419-018-1447-x>
- [17] D. Čakmak, Z. Tomičević, H. Wolf, Ž. Božić,  $\mathcal{H}_2$  optimization and numerical study of inerter-based vibration isolation system helical spring fatigue life, *Archive of Applied Mechanics* 89(7) (2019) 1221–1242. <https://doi.org/10.1007/s00419-018-1495-2>
- [18] D. Čakmak, Z. Tomičević, H. Wolf, Ž. Božić, D. Semenski, I. Trapić, Vibration fatigue study of the helical spring in the base-excited inerter-based isolation system, *Engineering Failure Analysis* 103 (2019) 44–56. <https://doi.org/10.1016/j.engfailanal.2019.04.064>
- [19] A.E.H. Love, *A Treatise on the Mathematical Theory of Elasticity*, Fourth Edition, Dover Publications, New York, 1944.
- [20] J. Kruzelecki, M. Życzkowski, On the concept of an equivalent column in the stability problem of compressed helical springs, *Ingenieur-Archiv* 60(6) (1990) 367–377. <https://doi.org/10.1007/BF00542566>
- [21] O. Göhner, Schubspannungsverteilung im Querschnitt einer Schraubenfeder, *Ingenieur-Archiv* 1(5) (1930) 619–644. <https://doi.org/10.1007/BF02079874>

- [22] O. Göhner, Die Berechnung Zylindrischer Schraubenfedern, *Zeitschrift des Vereines Deutscher Ingenieure* 76(11) (1932) 269–272.
- [23] P. Henrici, On Helical Springs of Finite Thickness, *Quarterly of Applied Mathematics* 13(1) (1955) 106–110. <https://doi.org/10.1090/qam/69006>
- [24] V. Kobelev, *Durability of Springs*, Springer, Cham, 2018.  
<https://doi.org/10.1007/978-3-319-58478-2>
- [25] W.R. Berry, Practical Problems in Spring Design, *Proceedings of the Institution of Mechanical Engineers* 139(1) (1938) 431–524.  
<https://doi.org/10.1243/PIME PROC 1938 139 017 02>
- [26] S.P. Timoshenko, J.N. Goodier, *Theory of Elasticity*, Second Edition, McGraw-Hill Book Co., New York, 1951.
- [27] H. Yazdani Sarvestani, A.H. Akbarzadeh, Thick isotropic curved tubes: three-dimensional stress analysis, *Archive of Applied Mechanics* 87(6) (2017) 927–947.  
<https://doi.org/10.1007/s00419-016-1223-8>
- [28] DIN EN 2089-1-1963-01, Helical springs made from round wire and rod - Calculation and design of Compression springs, 1963.
- [29] DIN EN 2089-1-1963-02, Helical springs made from round wire and rod - Calculation and design of Tension springs, 1963.
- [30] Y. Lin, A.P. Pisano, General Dynamic Equations of Helical Springs With Static Solution and Experimental Verification, *Journal of Applied Mechanics* 54(4) (1987) 910–917.  
<https://doi.org/10.1115/1.3173138>
- [31] T. Sumigawa, S. Chen, T. Yukishita, T. Kitamura, In situ observation of tensile behavior in a single silicon nano-helix grown by glancing angle deposition, *Thin Solid Films* 636 (2017) 70–77. <https://doi.org/10.1016/j.tsf.2017.05.036>
- [32] D.A. Antartis, R.N. Mott, I. Chasiotis, Silicon nanosprings fabricated by glancing angle deposition for ultra-compliant films and interfaces, *Materials and Design* 144 (2018) 182–191. <https://doi.org/10.1016/j.matdes.2018.02.017>
- [33] W.M. Huang, B. Yang, Y.Q. Fu, *Polyurethane Shape-Memory Polymers*, CRC Press, Boca Raton, 2012.
- [34] DIN EN 13906-1, Cylindrical helical springs made from round wire and bar - Calculation and design - Part 1: Compression springs, Beuth Verlag, Berlin, 2002.
- [35] DIN EN 13906-2, Cylindrical helical springs made from round wire and bar - Calculation and design - Part 2: Extension springs, Beuth Verlag, Berlin, 2002.
- [36] M. Shimoseki, T. Hamano, T. Imaizumi, *FEM for Springs*, Springer-Verlag, Berlin, 2003.  
<https://doi.org/10.1007/978-3-662-05044-6>
- [37] Dassault Systèmes, Abaqus 6.9 User's guide and theoretical manual, Hibbitt, Karlsson & Sorensen, Inc., Providence, RI, 2009.
- [38] Dassault Systèmes, Catia V5R19 Documentation: Finite Element Reference Guide, Vélizy-Villacoublay, France, 2007.
- [39] R. Rivera, A. Chiminelli, C. Gómez, J.L. Núñez, Fatigue failure analysis of a spring for elevator doors, *Engineering Failure Analysis* 17(4) (2010) 731–738.

<https://doi.org/10.1016/j.engfailanal.2009.08.018>

- [40] S.G. Keller, A.P. Gordon, Equivalent stress and strain distribution in helical compression springs subjected to bending, *Journal of Strain Analysis for Engineering Design* 46(6) (2011) 405–415. <https://doi.org/10.1177/0309324711410128>
- [41] D. Pastorčić, G. Vukelić, Ž. Božić, Coil spring failure and fatigue analysis, *Engineering Failure Analysis* 99 (2019) 310–318. <https://doi.org/10.1016/j.engfailanal.2019.02.017>
- [42] D.F. Caballero, J.M.M. Guijosa, V.R. de la Cruz, Generalized spiral torsion spring energetic model, *Archive of Applied Mechanics* 88 (2018) 999–1008. <https://doi.org/10.1007/s00419-018-1354-1>
- [43] V. Yıldırım, Exact determination of the global tip deflection of both close-coiled and open-coiled cylindrical helical compression springs having arbitrary doubly-symmetric cross-sections, *International Journal of Mechanical Sciences* 115-116 (2016) 280–298. <https://doi.org/10.1016/j.ijmecsci.2016.06.022>
- [44] V. Yıldırım, Axial Static Load Dependence Free Vibration Analysis of Helical Springs Based on the Theory of Spatially Curved Bars, *Latin American Journal of Solids and Structures* 13(15) (2016) 2852–2875. <https://doi.org/10.1590/1679-78253123>
- [45] S.P. Timoshenko, On the Correction for Shear of the Differential Equation for Transverse Vibrations of Prismatic Bars, *Philosophical Magazine* (Series 6) 41(245) (1921) 744–746. <https://doi.org/10.1080/14786442108636264>
- [46] S.P. Timoshenko, On the Transverse Vibrations of Bars of Uniform Cross-Section, *Philosophical Magazine* (Series 6) 43(253) (1922) 125–131. <https://doi.org/10.1080/14786442208633855>
- [47] J.R. Hutchinson, Shear Coefficients for Timoshenko Beam Theory, *ASME Journal of Applied Mechanics* 68(1) (2001) 87–92. <https://doi.org/10.1115/1.1349417>
- [48] T. Kaneko, On Timoshenko's correction for shear in vibrating beams, *Journal of Physics D: Applied Physics* 8(16) (1975) 1927–1936. <https://doi.org/10.1088/0022-3727/8/16/003>
- [49] T. Kaneko, An experimental study of the Timoshenko's shear coefficient for flexurally vibrating beams, *Journal of Physics D: Applied Physics* 11(14) (1978) 1979–1988. <https://doi.org/10.1088/0022-3727/11/14/010>
- [50] G.R. Cowper, The Shear Coefficients in Timoshenko's Beam Theory, *ASME Journal of Applied Mechanics* 33(2) (1966) 335–340. <https://doi.org/10.1115/1.3625046>
- [51] C.L. Dym, Consistent derivations of spring rates for helical springs, *ASME Journal of Mechanical Design* 131(7) (2009) 071004-1–5. <https://doi.org/10.1115/1.3125888>
- [52] J.W. Nicholson, J.G. Simmonds, Timoshenko Beam Theory Is Not Always More Accurate Than Elementary Beam Theory, *Journal of Applied Mechanics* 44(2) (1977) 337–338. <https://doi.org/10.1115/1.3424048>
- [53] D. Pearson, W.H. Wittrick, An exact solution for the vibration of helical springs using a Bernoulli-Euler model, *International Journal of Mechanical Sciences* 28(2) (1986) 83–96. [https://doi.org/10.1016/0020-7403\(86\)90016-0](https://doi.org/10.1016/0020-7403(86)90016-0)